INTERNATIONAL JOURNAL
OF
PHARMACEUTICAL SCIENCES
AND
RESEARCH

MOLECULAR MODELLING AND MOLECULAR DYNAMICS STUDIES OF SPECT PROTEIN OF *PLASMODIUM FALCIPARUM* AND *IN SILICO* SCREENING OF LEAD COMPOUNDS

Supriya Srivastava [1], Seneha Santoshi [1], Balwant Kishan Malik [2] and Puniti Mathur [*1]

Centre for Computational Biology and Bioinformatics [1], Amity Institute of Biotechnology, Amity University Noida - 201313, Uttar Pradesh, India.
Department of Biotechnology [2], Sharda University, Greater Noida - 201306, Uttar Pradesh, India.

ABSTRACT: Malaria has been a major life threatening mosquito borne disease. Unavailability of any effective vaccine and recent emergence of multi drug resistant strains of malarial pathogen *Plasmodium falciparum* continues to cause persistent deaths in the tropical and sub-tropical region. As a result, there is a growing demand for new targets for more effective anti-malarial drugs. A novel microneme protein, named sporozoite microneme protein essential for cell traversal (SPECT), is produced by the liver-infective sporozoite of the malarial parasite. In the present study, the 3D conformation of *Plasmodium falciparum* SPECT (*Pf*SPECT) protein was predicted using homology modelling and refined by 50 nanoseconds of MD simulation. The overall quality of the model was validated using PROCHECK and ERRAT. The PROCHECK results showed 91.4% of backbone angles were in the allowed region and ERRAT score of 85.9% suggested a high quality model. All docking calculations were performed using the "Extra Precision" (XP) mode of Glide docking. A database of 2,76,784 biogenic compounds was used for virtual screening, out of which 164 were identified as hits. Further, these compounds were analysed on the basis of docking and MM-GBSA scores and per residue interactions calculated. Molecular dynamics simulation studies were performed on two best protein-ligand complexes to check their stability. Ligand 1, ZINC03851216 depicted a stable hydrogen bond with Asn 99 residue on the protein and the complex stabilized after 10ns during the 50ns simulation time. Our data shows compelling indication that proposed ligands hold considerable potential for further experimental evaluation.

INTRODUCTION: Malaria continues to be a major parasitic disease affecting a large population in tropical and subtropical countries and causing 600,000 deaths every year [1, 2]. The infected female anopheles mosquito bites the human host and introduces the sporozoite form of the protozoan parasite into the dermis.

The sporozoites navigate through various host cell barriers in the dermis to enter blood circulation by displaying various modes of motility such as gliding, host cell traversal and transmigration between cells [3 - 6]. These highly motile sporozoites enter the liver lobules through the circulatory system comprising of hepatic artery, arterioles and sinusoidal capillaries. Inside the liver, the sporozoites exit the blood vessels displaying a range of motility and traversal through different cell types such as Kuppfer and endothelial cells. Finally, the sporozoites traverse and invade the hepatocytes and develop within a parasitophorous vacuole into exoerythrocytic forms (EEF) [7 - 9].

The EEFs mature into merozoites which exit the liver parenchyma, enter the blood stream and further infect erythrocytes leading to clinical manifestation of malaria. Almost all efforts to find newer, safe and effective drugs for malaria have been restricted to the cyclic blood stage of the parasite. However the asymptomatic liver stage, which the parasite goes through only once in its life history presents a less-explored opportunity for developing drugs, which could hit new targets, prevent pathology and also be used in highly desirable malaria eradication campaigns [10].

Recent studies have revealed a few drug targets in the pre erythrocytic or liver stage of the parasite [10, 11]. Of particular interest is the phenomenon of host cell traversal by the parasite [6, 13]. Cell traversal involves entry of sporozoite into a host cell, transit through the host cell cytosol, and finally exit from the host cell plasma membrane [3, 12]. Entry and apparently exit require the formation of a pore in the host cell plasma membrane, resulting in membrane wound that causes necrosis in most cases. In some of the instances wound is resealed and the cell persists [3, 5 - 15]. Recent studies on *P. yoelii* and *P. berghei* reveal that sporozoites traverse hepatocytes inside transient vacuoles that precede the formation of parasitophorous vacuole. The sporozoites initially invade cells inside transient vacuoles by an active moving junction [16-17] independent process that does not require vacuole membrane remodeling or release of parasite secretory organelles typically involved in invasion. Sporozoites use pH sensing and sporozoite microneme protein essential for cell traversal 2 (SPECT2) to exit these vacuoles and avoid degradation by host lysosomes [6, 18].

The important parasite proteins required for cell traversal include SPECT (sporozoite microneme protein essential for cell traversal) [13], SPECT2 (also known as perforin like protein 1, PLP-1) [19 - 20]. SPECT and SPECT2 are structurally unrelated secretory proteins. Though SPECT and SPECT2 were initially thought to facilitate wounding of the host cell membrane upon entry [11, 18], *P. berghei* and *P.yoelii* parasites lacking these proteins [15 - 16] can still readily enter hepatocytes. However these mutants cannot exit the vacuole including transient vacuoles or even the host cell [16]. In *Plasmodium berghei*, both of these proteins have been studied in

detail. Both proteins have signal sequences and are localized to micronemes, secretory organelles at the apical end of sporozoites [23]. The sequence of of *P. berghei* SPECT2 (*Pb*SPECT2) suggests that it has a direct role in pore formation. This protein of 800 amino acids has a central domain of 330 amino acids that has homology to pore-forming proteins, namely those belonging to the membrane attack complex / perforin (MACPF) and cholesterol-dependent cytolysin (CDC) family [12 - 15]. MACPF / CDC proteins are synthesized as soluble proteins and are triggered to undergo a conformational change that promotes insertion and pore formation in target membranes. Recombinant *P. falciparum* SPECT2 has been shown to have an important role in calcium dependent release of merozoites from human erythrocytes [24].

The exact function of SPECT in cell traversal remains unclear. The crystal structure of *Pb*SPECT, an approximately 25 kD protein has been recently published [23]. The structure reveals that the protein forms a four helix bundle, with the rare feature of having all of them in parallel or anti-parallel alignment. The angle between helices range between 1-8 degree. This is a rare arrangement of four helix bundle proteins. The packing of side chains arrangements in tilted helices accords a stable structure to the protein. However, in the present case unfavorable packing of side chains leads to a labile conformation. It is proposed that *Pb*SPECT could be triggered to undergo a conformational transition from soluble to membrane associated or inserted form. Homologs of *Pb*SPECT have been found only in the genomes of various Plasmodium species, including *P. falciparum* [23]. These proteins have 40% sequence identity, suggesting that they share a common structure and mode of action. As *Plasmodium falciparum* accounts for the majority of malarial infections in human and is responsible for virtually all malaria related mortality worldwide [1], it would be interesting and relevant to study the *P. falciparum* SPECT protein.

In the present study, the three-dimensional structure of *P. falciparum* SPECT, *Pf*SPECT was predicted using homology modelling [25] and further refined using molecular dynamics simulation. Biogenic compounds of the ZINC database were docked on the predicted binding site of this protein.

The molecules showing reasonable binding affinity were further evaluated using molecular dynamics of the protein-ligand complex and interactions between the protein and ligands studied.

MATERIAL AND METHODS:

Structural Modelling of *Pf*SPECT Protein: As the crystal structure of *Pf*SPECT is not yet available, the 3D structure of the protein was predicted using knowledge based homology modelling method. The amino acid sequence of *Plasmodium falciparum* (isolate 3D7) with accession number XP_001350146 was used for structure prediction. Template search for homology modelling was performed using BLAST and HHBlits against the SWISS-MODEL template library (SMTL). The target sequence was submitted to BLAST [26] against the protein sequences contained in the template library of SWISS-MODEL. Seven templates were found against the target sequence. HHblits profile was built after which 1iteration of HHblits was performed against nr20 [27]. Total ten templates were found after screening against all profiles of the SMTL. With the target template alignment feature, quality of the template was predicted. Finally *Pb*SPECT (PDB ID: 4u5a) was selected as the template for model development. Promod-II was used to generate model based on target template alignment, conserved coordinates between the target and template were copied from the template to the model. Using a fragment library, insertions and deletions were remodelled, side chains were then rebuilt and finally, the geometry of the resulting model was regularized.

Protein Refinement and Validation: Energy minimization of the modelled protein was performed using Macromodel (version 9.9, Schrodinger) and OPLS 2005 force field with PRCG algorithm using 1,000 steps of minimization and energy gradient of 0.001. The total energy of the energy minimized structure was calculated and the overall quality was evaluated using PROCHECK [28] and ERRAT [29].

The generated protein structure was further refined by performing a 50ns (nanoseconds) molecular dynamics simulation using desmond through the multistep MD protocols of Maestro, (version 10.3, Schrödinger). The initial steps of MD simulations were performed by using OPLS 2005 molecular mechanics force field. The protein was solvated in cubic box with a dimension of 20Å using simple point charge water molecules, which were then replaced with 8 Na$^+$ counterions for electro-neutrality. A total of 5,000 frames were generated in the MD trajectories, out of which the last 2,000 frames were used to generate structure of the *Pf*SPECT protein. The total energy of the simulated model was calculated and the overall quality was again validated using different software used previously.

Ligand Preparation: A library of 2,76784 biogenic compounds from ZINC database, a freely available database of commercially available compounds, was chosen for screening. This library is composed of molecules of biological origin. The advantage of using such screening libraries is that they are more likely to provide far richer and denser hits that one would expect by screening synthetic compounds alone. The structures in the library were prepared for further analysis using LigPrep, version 3.5, Schrödinger. For each structure, proper bond orders were assigned and different tautomeric forms were produced. All possible stereoisomers for each ligand were generated by the program (default value 32). These structures were further used for performing interaction studies with the protein.

Molecular Docking: Protein ligand docking studies were carried out based on the MD simulated structure of *Pf*SPECT which was prepared using multi-step Schrödinger's protein preparation wizard before proceeding for docking calculations. As the binding site of the protein was not known, it was predicted using Sitemap (version 3.6, Schrödinger). Molecular docking calculation for all the compounds, to determine the binding affinity of *Pf*SPECT binding site, was performed using Glide (version 6.8, Schrödinger). At the centroid of protein binding site receptor grid was generated. A box of size 10 Å x 10 Å x 10 Å was defined in the center of binding site for the binding of docked ligand and to occupy all the atoms of the docked poses one more enclosing box of 12 Å x 12 Å x 12 Å was also defined. The structure was studied for interaction with the entire library of biogenic compounds selected from the ZINC database. 276784 compounds were screened by different

filters (Qikprop, reactive, Lipinski's rule of five) and selected compounds obtained were used as input for HTVS in the first level of screening. Compounds screened after using HTVS were further used in next level for molecular docking calculations using "Standard Precision" (SP) algorithm. Compounds selected after SP docking were further refined using "Extra Precision" (XP) algorithm of Glide Docking. On the basis of XP docking scores, some compounds were selected for further analysis. The binding affinity was calculated based on MMGBSA (Molecular Mechanics Generalised Born Surface Area) using Prime, (version 4.1, Schrödinger). The interaction studies using molecular docking and MMGBSA revealed appreciable docking scores and $\Delta G_{bind.}$

Molecular Dynamics Simulation: In order to further refine the results, MD simulation of the docked complexes was performed. We have selected two compounds from the entire list, which have shown the best (lowest) binding energy with the protein, for MD simulation. Molecular dynamics (MD) simulation for docked complexes of *Pf*SPECT was performed using Desmond 2.2 implemented in Schrödinger package with 50 ns simulation time. The initial steps of MD simulations were done by applying OPLS 2005 molecular mechanics force field, 10067 water molecules were placed with the ligand-receptor complex with SPC (simple point charge) water model. System was neutralized with $8Na^+$ counter ions, SHAKE algorithm was used to constrain the geometry of water molecules and heavy atom bond lengths with hydrogens. Electrostatic interactions using particle mesh ewald (PME) method and periodic boundary conditions (PBC) were used.

The full system was simulated through the multistep MD protocols of Maestro, version 10.3. Briefly, full system minimization with restraints on solute was performed for maximum 2000 iterations of a hybrid of the steepest descent and the limited memory Broyden - Fletcher - Gold farb-Shanno (LBFGS) algorithms, with a convergence threshold of $5.0 kcal/mol/Å^2$. Similar minimization without any restraints was performed with a convergence threshold of $kcal/mol/Å^2$. Simulations restraining non hydrogen solute atoms were performed in the NPT ensemble (constant number of atoms N, pressure P and temperature T) for 12ps simulation

time and temperature of 10K. Further, NPT ensemble for a simulation time of 24ps restraining all non hydrogen solute atoms (temperature 300K) and NPT ensemble, without restraints, for a simulation time of 24ps (temperature 300K) was performed to relax the system.

The relaxed system was simulated for a period of 10000ps with a time step of 2 femtosecond (fs), NPT ensemble using a Berendsen thermostat at 310 K and velocity resampling for every 1ps. Trajectories after every 4.8ps were recorded. Total of about 10000 frames were generated. Energy fluctuations and RMSD of the complex in each trajectory were analyzed with respect to simulation time. The backbone and side chain root mean square fluctuations (RMSF) of each residue of *Pf*SPECT protein were monitored for consistency. The inter-molecular interactions were assessed for stability of the docking complex.

RESULTS AND DISCUSSION:
Homology Modelling of *Pf*SPECT: Homology modelled structure of *Pf*SPECT protein was constructed from crystal structure template of *Pb*SPECT (PDB ID: 4u5a), as shown in **Fig. 1A**. Validation of the protein was performed by saves server. The PROCHECK results showed 77.7% of backbone angles were in allowed regions with G-factor of 21.7. Ramachandran plot analysis revealed no residue in the disallowed region, 0.6% residues in additionally allowed regions and no residues in generously allowed regions.
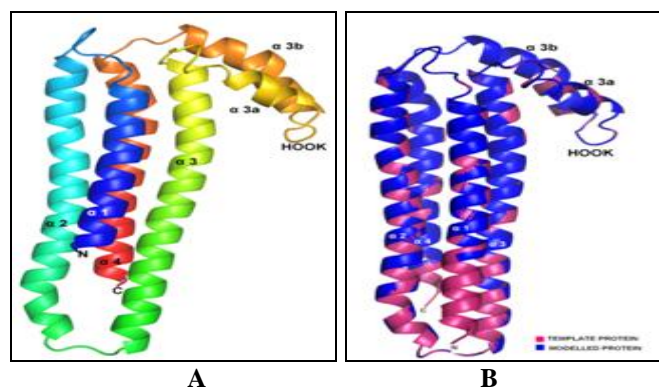

A   **B**

FIG. 1: STRUCTURE OF MODELLED *Pf*SPECT PROTEIN. (A) RIBBON REPRESENTATION OF THE FOUR-HELIX BUNDLE STRUCTURE OF *Pb*SPECT, WITH INDIVIDUAL α-HELICES IN DIFFERENT COLORS. (B) SUPERIMPOSED STRUCTURES OF MODELLED *Pf*SPECT PROTEIN WITH THE TEMPLATE *Pb*SPECT PROTEIN

In order to further ascertain the quality of the model generated, the energy of the generated model was calculated which was found out to be -50867.023kJ/mol. Predicted model was super-imposed with template model of *Pb*SPECT and rmsd was found to be 1.062 Å as shown in **Fig. 1b**.

Model Refinement and Energy Minimization: The developed *Pf*SPECT model was further refined by performing a MD simulation with 50ns simulation time using desmond 2.2 implemented in Schrödinger package. To evaluate the structure deviation, RMSD was calculated during the simulation based on initial backbone coordinates as represented in **Fig. 2A**.

All protein frames are first aligned on the reference frame backbone, and then the RMSD was calculated based on the atom selection. RMSD plot revealed that relative fluctuation of the RMSD was very stable after 40ns thus showing the stability of the system. Furthermore, the root mean structure fluctuation (RMSF) of the amino acid residues was calculated to reveal the flexibility of the residues. Plot in the **Fig. 2B** shows peaks which indicate areas of the protein that fluctuate the most during the simulation. Secondary structure elements like alpha helices were usually more rigid than the unstructured part of the protein, and thus fluctuate less than the loop regions.
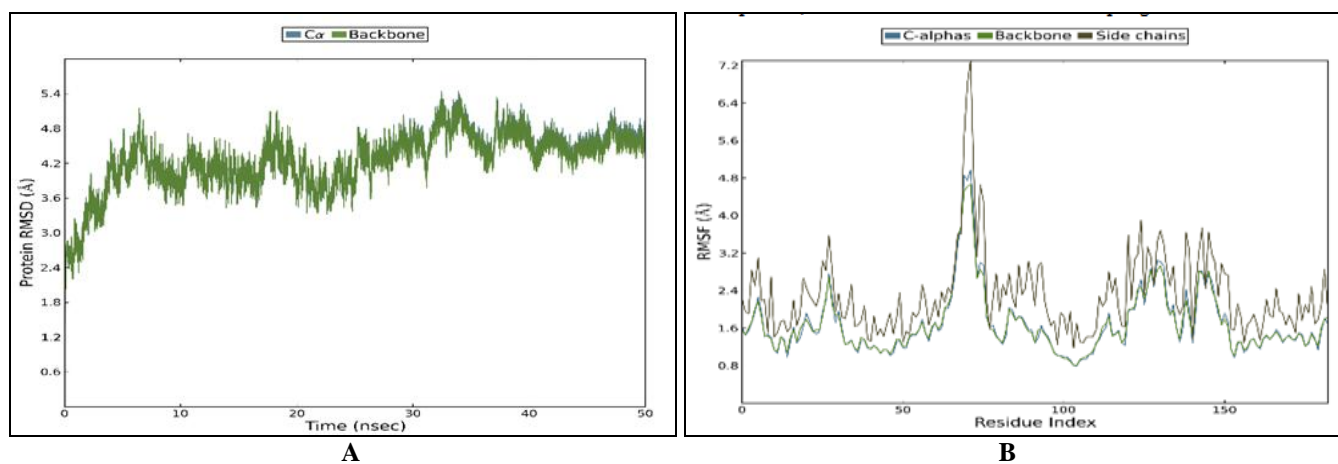

FIG. 2: 50ns MOLECULAR DYNAMICS SIMULATIONS RUN OF *Pf*SPECT PROTEIN FOR REFINEMENT OF STRUCTURE (A) RMSD OF HEAVY ATOMS AND BACK BONE ATOMS. (B) PROTEIN RMSF SHOWING FLEXIBILITY OF THE RESIDUES

In order to check the quality of the structure, energy of the simulated model was calculated. The molecular dynamics simulation reduced the potential energy of *Pf*SPECT model from -50867.023 kJ/mol to -52162.293 kJ/mol, which indicated an improved quality of the model.
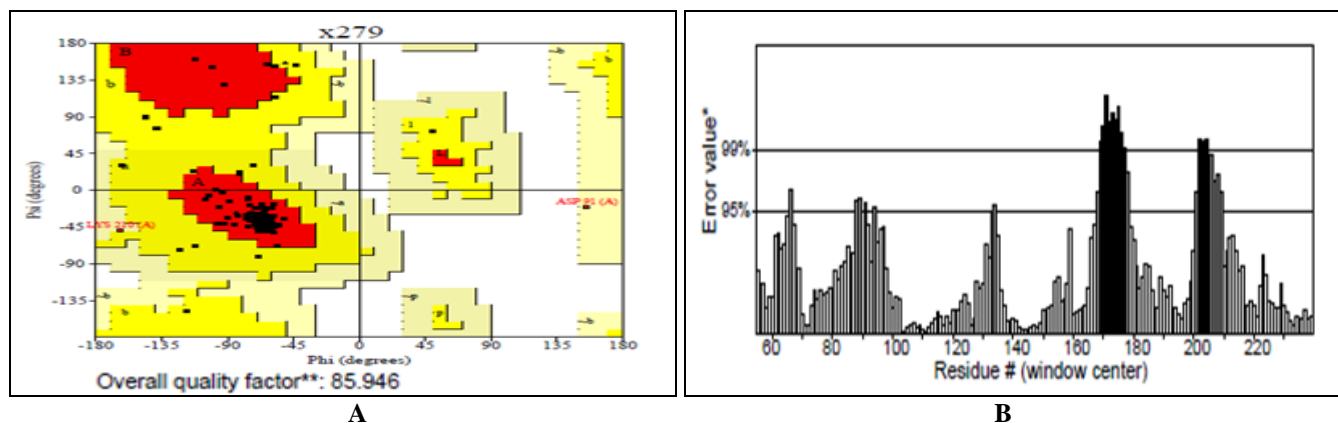

FIG. 3: VALIDATION OF MD SIMULATED STRUCTURE OF *Pf*SPECT PROTEIN (A): RAMACHANDRAN PLOT WHICH SHOWS 91.4% OF BACKBONE ANGLES WERE IN ALLOWED REGIONS WITH G-FACTORS OF -0.16. REVEALING NO RESIDUE IN THE DISALLOWED REGION, 7.6% RESIDUES IN ADDITIONALLY ALLOWED REGIONS AND 1.1 % RESIDUES IN GENEROUSLY ALLOWED REGIONS (B): ERRAT SHOWING OVERALL QUALITY FACTOR: 85.946

The MD simulated structure was further evaluated using PROCHECK and ERRAT. The PROCHECK results showed 91.4% of backbone angles were in allowed regions with G-factors of -0.16. Ramachandran plot analysis revealed no residue in the disallowed region, 7.6% residues in additionally allowed regions and 1.1 % residues in generously allowed regions shown in **Fig. 3a** [30]. The ERRAT score was 85.9% that is within the range of high quality model shown in **Fig. 3b**. Thus the overall quality of the structure generated by homology modelling was very good and the refined structure with minimum energy was further used to perform molecular docking studies.

Analysis of Predicted *Pf*SPECT Binding Site:
The binding site of *Pf*SPECT was computationally predicted to analyze the protein for interaction with lead molecules. This was performed using Sitemap, (version 3.6, Schrödinger) and the results obtained have been listed in **Table 1**.

TABLE 1: PREDICTED BINDING SITES OF *Pf*SPECT WITH SITE SCORES

Site ID	Site Score (a.u)	Drug ability Score (a.u)	Volume (Å)^3
1	1.171	1.240	378.6
2	0.736	0.727	135.1
3	0.724	0.753	83.349
4	0.670	0.652	65.513
5	0.637	0.588	85.407

Five sites were predicted as shown in **Fig. 4a**. The sitemap score ranged from 0.637 to 1.171 and as per the standard binding sitemap score of greater than 0.8 [31], we have selected site1, with the best sitemap score *i.e.* 1.171, with drug ability score 1.240 and volume 378.6 (Å)^3 for further interaction studies. The residues involved in the selected site were V11, S14, M15, V18, L19, T22, A24, S25, L26, V29, S30, H32, V33, I37, Y40, S41, I44, L48,

L92, K93, L95, E96, N99, I102, K103, I106, I107, Y110, G111, N112, K113, N145, D148, K150, E151, L154, I158, N161, Y162, K164, F165 and L169. We found out that the area covered by predicted binding site in *Pf*SPECT was similar to the reported binding pocket and cavity present in the crystal structure of the *Pb*SPECT as shown in **Fig. 4b** [23]. The positions of some of the residues in the predicted binding site of PfSPECT were common with those in *Pb*SPECT pocket and cavity, such as 99, 102, 164, 169.
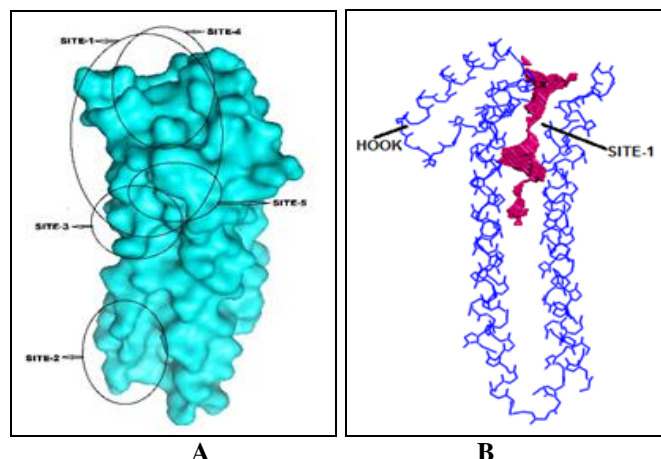

FIG. 4: (A) DIFFERENT PREDICTED BINDING SITES OF THE *Pf*SPECT PROTEIN (B) STEREOVIEW OF THE INTERIOR CAVITY OF SITE 1 IN *Pf*SPECT DEPICTED AS STICKS AND THE MAIN CHAIN OF SPECT PROTEIN AS LINES

Molecular Docking Calculations of *Pf*SPECT Protein: The interaction of the *Pf*SPECT with the various ligands was studied using molecular docking calculations using Glide, (version 6.8, Schrödinger). The Glide docking program validates different positions, orientations and conformation of ligands in the binding site in a systematic manner and returns the best docked poses of various ligands in the binding pocket.

TABLE 2: GLIDE ENERGY, DOCKING SCORE AND MMGBSA (ΔG$_{bind}$) SCORE OF SELECTED LIGANDS

S. No.	Zinc Id	Glide Energy	Docking Score	Δg$_{bind}$
1	ZINC03851216	-36.078	-10.669	-90.092
2	ZINC0513454	-29.108	-10.544	-88.092
3	ZINC77257422	-25.172	-9.285	-84.161
4	ZINC03851232	-32.918	-9.499	-83.553
5	ZINC03978926	-32.84	-9.669	-80.974
6	ZINC05124607	-34.038	-9.524	-80.195
7	ZINC00518290	-31.536	-9.968	-78.599
8	ZINC12496555	-36.513	-10.289	78.337
9	ZINC03847760	-34.181	-9.309	-78.007
10	ZINC15255743	-22.767	-9.373	-77.402

164530 compounds were used as input for HTVS in the first level of screening. 16453 compounds were screened using HTVS and further used in next level for molecular docking calculations using "Standard Precision" SP. 1645 compounds selected after SP docking were further refined using "Extra Precision" (XP) algorithm of Glide Docking. On the basis of XP docking scores, 164 compounds were selected for further analysis. The 10 compounds among the above, showing promising leads with appreciable docking scores in the range of -10.669 to -9.285 are shown in **Table 2**.

Binding Affinity Calculation: The binding affinity was further calculated to check binding free energy using MMGBSA. The interaction studies using molecular docking and MMGBSA revealed appreciable docking scores and ΔG_{bind}. **Table 2**

shows the selected best 10 compounds showing promising leads with appreciable docking score and a range of ΔG_{bind} score from -90.092 to -76.152 Kcal/mol. After analysing the binding mode, two ligands, ZINC03851216 as ligand-1 and ZINC0513454 named as ligand-2 were selected for further calculations. Analysis of binding mode of *Pf*SPECT showed hydrogen bonding (H-bond) patterns of both ligands from docked poses within binding pocket of *Pf*SPECT protein as shown in **Fig. 5a** and **b**. Only one H-bond was formed between ligand-1 and Asn-99 at the binding site. In case of ligand 2, one side chain hydrogen bond with Asn-99 and one main chain hydrogen bond with Met-15 could be seen in the binding pocket (**Fig. 5c** and **d**).
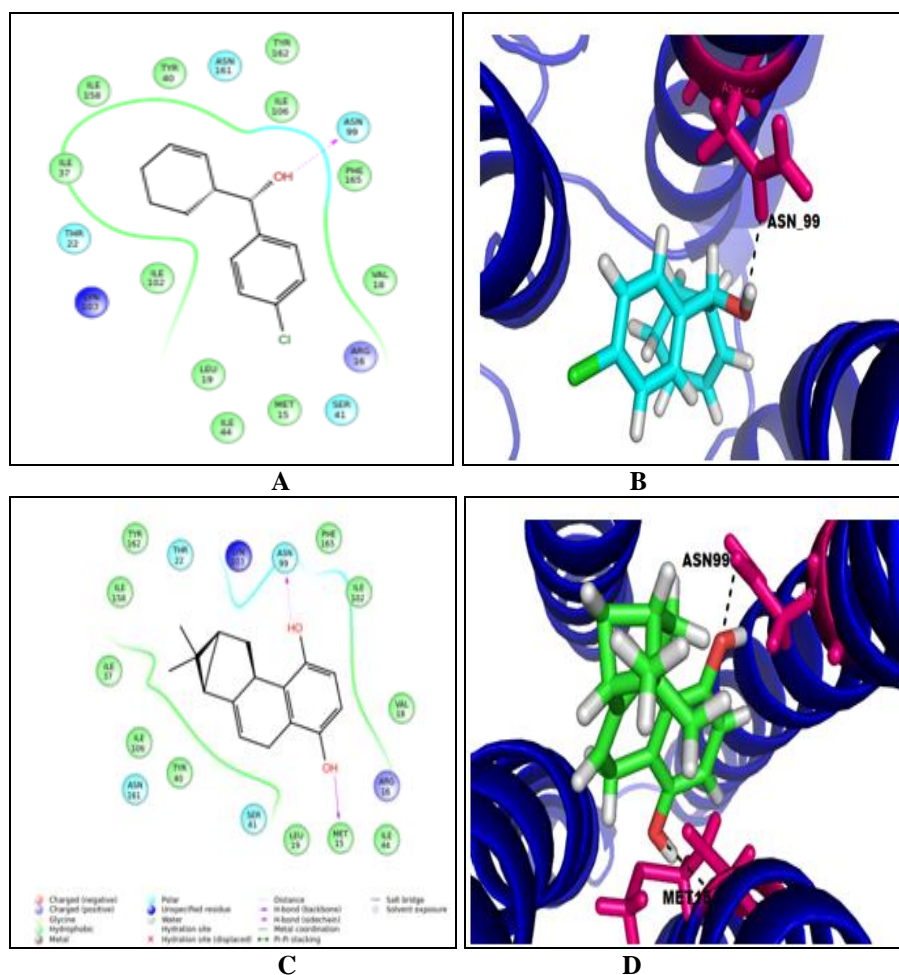

FIG. 5: (A) LIGAND INTERACTION WITH *Pf*SPECT PROTEIN SHOWING HYDROGEN BOND BETWEEN LIGAND-1 AND ASN-99 (B) 3-DIMENSIONAL STRUCTURE FITTING OF LIGAND-1 WITH THE BINDING SITE OF *Pf*SPECT PROTEIN SHOWING HYDROGEN BOND (C) LIGAND INTERACTION WITH *Pf*SPECT PROTEIN SHOWING HYDROGEN BOND BETWEEN LIGAND-2 AND ASN99 AND MET15 (D) 3-DIMENSIONAL STRUCTURE FITTING OF LIGAND-2 WITH THE BINDING SITE OF *Pf*SPECT PROTEIN SHOWING HYDROGEN BOND

Per Residue Energy Contribution: To understand the molecular basis of interaction of *Pf*SPECT with the selected ligands, we have calculated per residue van der Waals (E_{vdw}) and electrostatic (E_{ele}) energy contribution of amino acids within 12 Å of the docked ligands. The binding site amino acids showed significant contribution to the E_{vdw} and E_{ele} energy in both ligands 1 and 2 (**Fig. 6**). Specifically,

appreciable E_{ele} energy contribution was made by Asn-99 in case of both ligands 1 and 2 and Met-15 for only ligand 2. Significant E_{vdw} contribution was made by amino acids such as Phe 165, Tyr 162, Ile-158, Ile-102, Asn-99, Ile-44, Tyr-40, Leu-19, Met-15 in case of ligand 1. In case of ligand 2, three additional amino acids namely Ile-37 and Thr-22 also showed van der waals interactions.
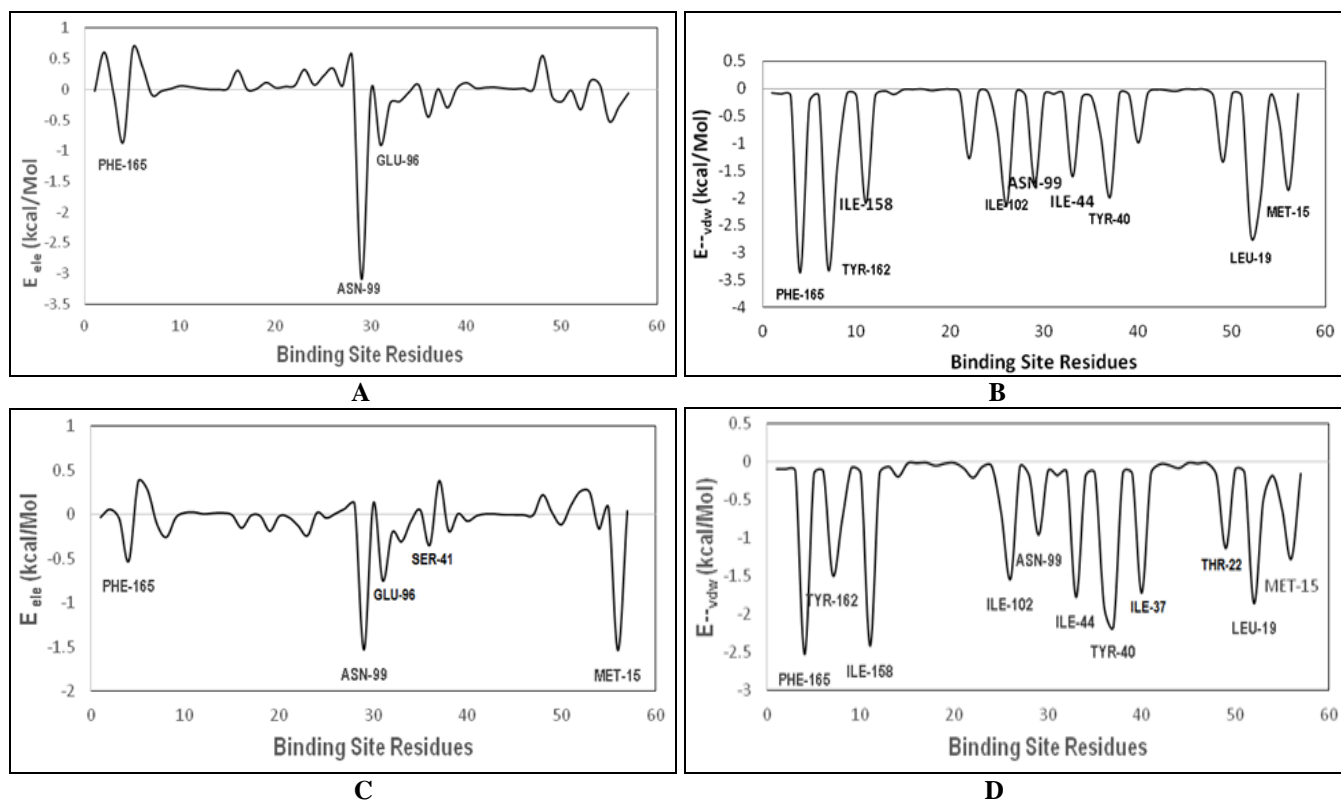

FIG. 6: GRAPH SHOWING PER RESIDUE ENERGY (A) E_{ele} OF LIGAND 1 (B) E_{vdw} OF LIGAND 1 (C) E_{ele} OF LIGAND 2 (D) E_{vdw} OF LIGAND 2

Molecular Dynamics Simulation: In order to check the stability of the docked ligands, we determined the preferred binding mode and binding affinity of these two best ligands with *Pf*SPECT by performing 50ns of MD simulations. The simulation shows binding interaction of the docking complex with system embedded with water molecules at normal temperature and pressure. For the complex of ligand 1 and protein, the RMSD plot revealed that the complex was relatively stable throughout the simulation time as it found stability after 10ns, shown in **Fig. 7a**. RMSD plot for second ligand (**Fig. 8a**) revealed that relative fluctuation of the RMSD was very stable after 35 ns thus showing the first ligand is more stable and well within the binding pocket of *Pf*SPECT than the second ligand. Analysis of post-

processing interaction was done to observe the ligand-protein binding interactions by analyzing the trajectory data obtained from the MD simulation. The timeline representation showed that Asn-99 and Asn-161 were stable in overall time with ligand 1 while Phe-165 and Met-15 were stable in overall time with ligand 2. Lower RMSF value was shown by the residues of the active site and alpha helical regions which indicated the stability of the regions (**Fig. 7b** and **8b**). The protein-ligand contacts were normalized over the course of the trajectory (**Fig. 7c** and **8c**). Ligand 1 depicted main chain hydrogen bond with Asn-161 and side chain hydrogen bond with Asn-99 as shown in Fig. 7d while ligand-2 showed a hydrogen bond with Met-15 and pi-pi stacking with Phe-165 as shown in **Fig. 8d**.
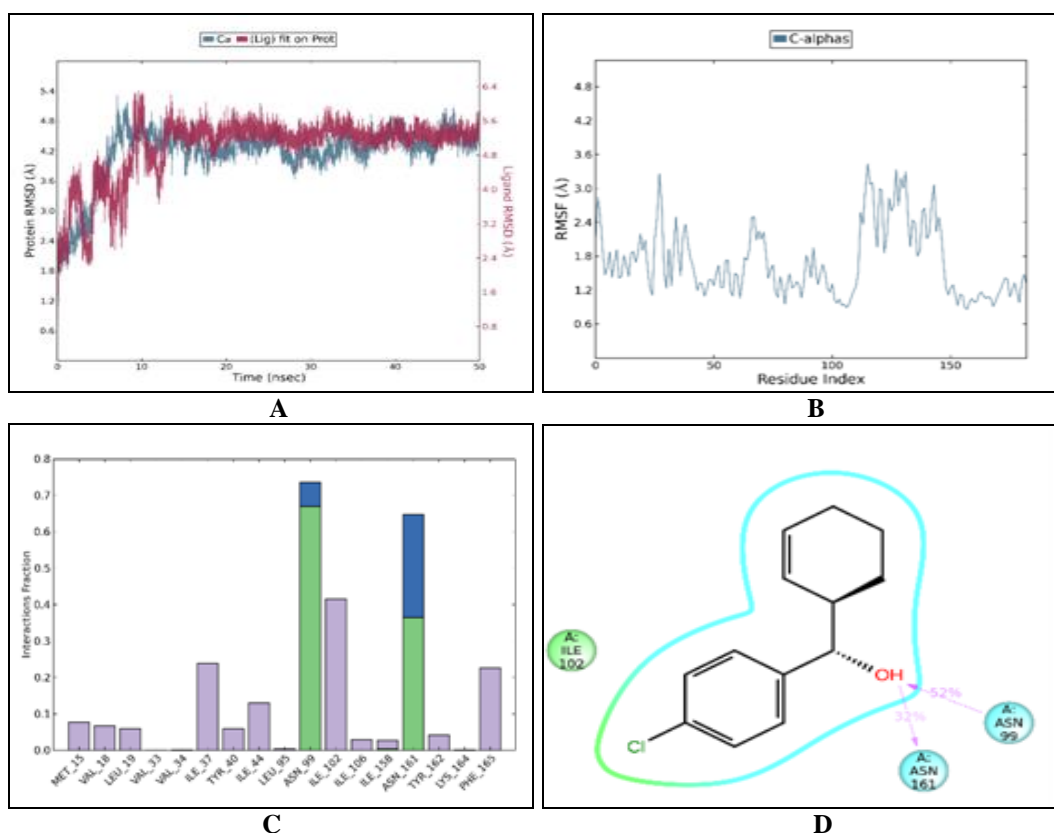
FIG. 7: INTERACTIONS OF *Pf*SPECT AND LIGAND 1 COMPLEX DURING 50ns MOLECULAR DYNAMICS SIMULATIONS RUN. A. RMSD OF HEAVY ATOMS AND BACK BONE ATOMS. B. PROTEIN RMSF C. PROTEIN LIGAND CONTACTS D. PROTEIN- LIGAND COMPLEX IN THE LAST TRAJECTORY SHOWING TWO HYDROGEN BOND
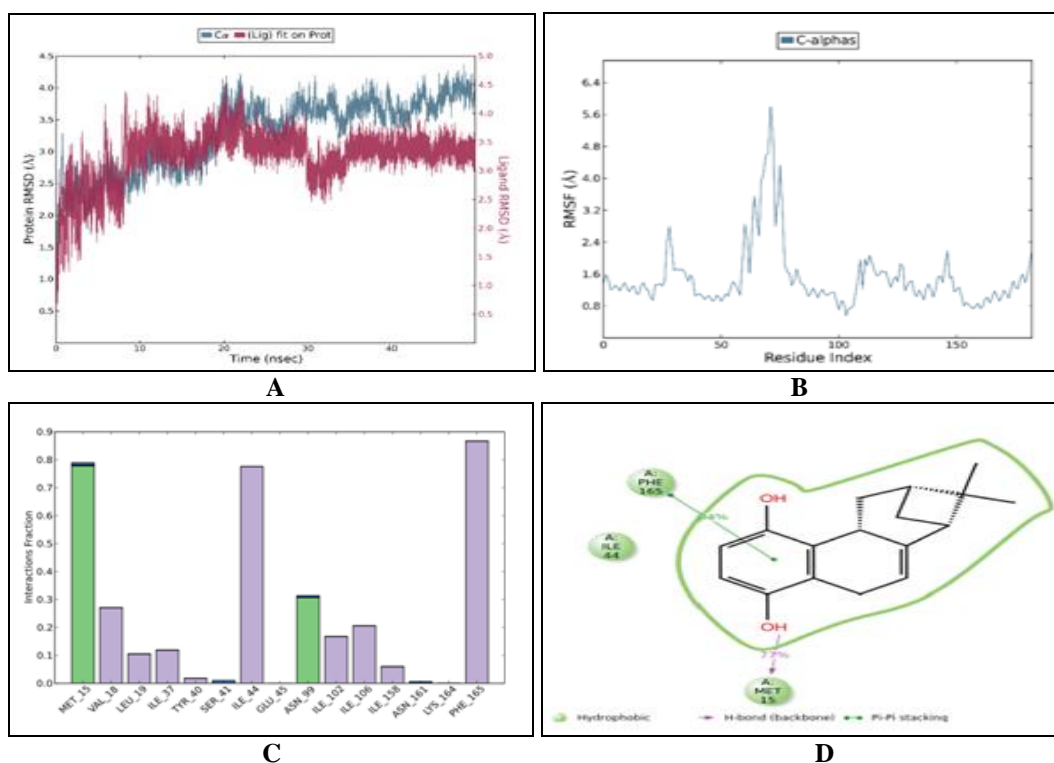

FIG. 8: INTERACTIONS OF *Pf*SPECT AND LIGAND 2 COMPLEX DURING 50ns MOLECULAR DYNAMICS SIMULATIONS RUN. A. RMSD OF HEAVY ATOMS AND BACK BONE ATOMS. B. PROTEIN RMSF C. PROTEIN LIGAND CONTACTS D. PROTEIN- LIGAND COMPLEX IN THE LAST TRAJECTORY SHOWING ONE HYDROGEN BOND

CONCLUSION: In conclusion, a good quality three-dimensional structure of *Pf*SPECT was determined using homology modelling and molecular dynamics simulations. Cα rmsd of 1.062 Å with the template protein *Pb*SPECT, Ramachandran plot showing 91.4% of backbone angles of *Pf*SPECT in the allowed regions and an ERRAT score of 85.9% further validated the quality of structure. A series of docking studies were performed and binding affinity of ligands with the protein evaluated. Two molecules, namely ZINC03851216 and ZINC0513454 showed appreciable docking scores and high affinity towards the binding site of the protein. Molecular dynamics simulations of these ligand-protein complexes depicted stability after 10ns and 35ns respectively.

These studies revealed hydrogen bonding interactions between the ligands and amino acids such as Asn-99, Met-15 and pi-pi interaction with Phe-165, which were conserved during a large period of the overall simulation time. It is therefore hypothesized that this study could be the basis for medicinal chemists to design newer compounds that may act as inhibitors of *Pf*SPECT and eventually interfere with the process of host cell traversal. Our findings may open the way for novel malaria transmission-blocking strategies that target molecules involved in sporozoite migration to the hepatocyte.

CONFLICT OF INTEREST: No potential conflict of interest was reported by the authors.

REFERENCES:

1. Cowman AF, Healer J, Marapana D and Marsh K: Malaria: Biology and Disease. Cell 2016; 167: 610-624.
2. WHO: The World Malaria Report http://www.whoint/ malaria/publications/ world malaria report 2015/report/en/ 2015.
3. Mota MM, Pradel G, Vanderberg JP, Hafalla JC, Frevert U, Nussenzweig RS, Nussenzweig V and Rodriguez A: Migration of Plasmodium sporozoites through cells before infection. Science 2001; (291)5501: 141-144.
4. Tavares J, Formaglio P, Thiberge S, Mordelet E, Van N and Rooijen: Role of host cell traversal by the malaria sporozoite during liver infection. J. Exp. Med. 2013; 210(5): 905–915.
5. Amino R, Giovannini D, Thiberge S, Gueirard P, Boisson B *et al*.: Host cell traversal is important for progression of the malaria parasite through the dermis to the liver. Cell Host Microbe 2008; 3(2): 88–96.
6. Yang SP and Boddey JA: Molecular mechanisms of host cell traversal by malaria sporozoites. Mol. BioSyst. 2017; 47(2-3): 129-136.
7. Sturm A, Amino R, Van de Sand C, Regen T, Retzlaff S, Rennenberg A, Krueger A, Pollok JM, Menard R and Heussler VT: Manipulation of host hepatocytes by the malaria parasite for delivery into liver sinusoids. Science 2006; 313(5791): 1287-90.
8. Amino R, Thiberge S, Martin B, Celli S, Shorte S, Frischknecht F and Ménard R: Quantitative imaging of Plasmodium transmission from mosquito to mammal. Nat. Med 2006; 12: 220–224.
9. Yamauchi LM, Coppi A, Snounou G and Sinnis P: *Plasmodium sporozoites* trickle out of the injection site. Cell Microbiol. 2007; 9: 1215–1222.
10. Derbyshire ER, Mota MM and Clardy J: The Next Opportunity in Anti-Malaria Drug Discovery: The Liver Stage. PLoS Pathog. 2011; 7(9): e1002178.
11. Mazier D, Rénia L and Snounou G: A pre-emptive strike against malaria's stealthy hepatic forms. Nature Rev. Drug Discov. 2009; 8: 854-864.
12. Vanderberg JP, Serena C and Michael JS: Plasmodium Sporozoite Interactions with Macrophages *in vitro*: a Video microscopic Analysis. J Eukaryot Microbiol. 1990; 37(6): 528-536.
13. Ishino T, Yano K, Chinzei Y and Yuda M: Cell-passage activity is required for the malarial parasite to cross the liver sinusoidal cell layer. PLoS Biol. 2004; 2(1): 77–84.
14. Formaglio P, Tavares J, Menard R and Amino R: Loss of host cell plasma membrane integrity following cell traversal by Plasmodium sporozoites in the skin. Parasitol. Int., 2014; 63(1): 237–244.
15. Frevert U, Engelmann S, Zougbede S, Stange J and Ng B: Intravital observation of *Plasmodium berghei* sporozoite infection of the liver. PLoS Biol. 2005; 3(6): e192.
16. Sibley LD: Intracellular Parasite Invasion Strategies. Science.2004;304(5668): 248-253.
17. Amino R, Giovannini D, Thiberge S, Gueirard P, Boisson B, Dubremetz JF, Prévost MC, Ishino T, Yuda M, Yuda M and Ménard R: Host Cell Traversal is Important for Progression of the Malaria Parasite through the Dermis to the Liver**.** Cell Host Microbe 2008; 3: 88–96.
18. Risco-Castillo V, Topçu S, Marinach C, Manzoni G, Bigorgne AE, Briquet S, Baudin X, Lebrun M, Dubremetz JF and Silvie O: Malaria Sporozoites Traverse Host Cells within Transient Vacuoles. Cell Host Microbe 2015; 18: 593–603.
19. Kaiser K, Matuschewski K, Camargo N, Ross J and Kappe SHI: Differential transcriptome profiling identifies Plasmodium genes encoding pre-erythrocytic stage-specific proteins, Mol. Microbiol. 2004; 51(5): 1365-2958.
20. Ishino T, Chinzei Y and Yuda M: A Plasmodium sporozoite protein with a membrane attack complex domain is required for breaching the liver sinusoidal cell layer prior to hepatocyte infection. Cell Microbiol 2005; 7(2): 199-208.
21. Aly ASI, Vaughan AM and Kappe1 SHI: Malaria Parasite Development in the Mosquito and Infection of the Mammalian Host. Annu Rev Microbiol. 2009; 63: 195-221.
22. Kariu T, Ishino T, Yano K, Chinzei Y and Yuda M: CelTOS, a novel malarial protein that mediates

transmission to mosquito and vertebrate hosts. Mol. Microbiol. 2006; 59(5): 1369–79.

23. Hamaoka BY and Ghosh P: Structure of the Essential Plasmodium Host Cell Traversal Protein SPECT1. PLoS One. 2014; 9(12): e114685.

24. Garg S, Agarwal S, Kumar S, Yazdani SS, Chitnis CE, Singh S: Calcium-dependent permeabilization of erythrocytes by a perforin-like protein during egress of malaria parasites. Nat. Commun. 2013; 4: 1736.

25. França TCC: Homology modeling: an important tool for the drug discovery. J. Biomol. Struct. Dynam. 2015; 33(8): 1780e93.

26. Guex N and Peitsch MC: Swiss-Model and Swiss-Pdb Viewer: an environment for comparative protein modelling. Electrophoresis. 1997; 18(15): 2714–2723.

27. Remmert M, Biegert A, Hauser A and Söding J: HHblits: lightning-fast iterative protein sequence searching by HMM-HMM alignment. Nat. Methods. 2011; 9: 173-5.

28. Laskowski RA, MacArthur MW, Moss DS and Thornton JM: Procheck: a program to check the stereo chemical quality of protein structures. J App. Crystal 1993; 26: 283–291.

29. Colovos C and Yeates TO: Verification of protein structures: patterns of non-bonded atomic interactions. Protein Sci. 1993; 2(9): 1511–1519.

30. Ramachandran GN, Ramakrishnan C and Sasisekharan V: Stereochemistry of polypeptide chain configurations. J. Mol. Biol. 1963; 7: 95–99.

31. Halgren TA: Identifying and characterizing binding sites and assessing drug ability. J. Chem. Inf. Model 2009; 49(2): 377–389.